



ELSEVIER

Biophysical Chemistry 87 (2000) 63–72

Biophysical  
Chemistry

www.elsevier.nl/locate/bpc

## Structure of a fusion peptide analogue at the air–water interface, determined from surface activity, infrared spectroscopy and scanning force microscopy

S.E. Taylor<sup>a</sup>, B. Desbat<sup>b</sup>, D. Blaudez<sup>c</sup>, S. Jacobi<sup>d</sup>, L.F. Chi<sup>d</sup>, H. Fuchs<sup>d</sup>,  
G. Schwarz<sup>a,\*</sup>

<sup>a</sup>Department of Biophysical Chemistry, Biocenter of the University, Klingelbergstr. 70, CH 4056 Basel, Switzerland

<sup>b</sup>Laboratoire de Physico-Chimie Moléculaire, Université Bordeaux I, F 33405 Talence, France

<sup>c</sup>Centre de Physique Moléculaire Optique et Hertzienne, Université Bordeaux I, F 33405 Talence, France

<sup>d</sup>Physikalisches Institut, Westfälische Wilhelms-Universität, Wilhelm-Klemm-Str. 10, D 48149 Münster, Germany

Received 27 March 2000; received in revised form 23 June 2000; accepted 24 June 2000

### Abstract

We have investigated a point mutant of the HIV-1 fusion peptide in a compressed monolayer at the air–water interface. A variety of surface sensitive techniques were applied to study structural features under conditions mimicking the hydrophobic/ hydrophilic environment of a biomembrane. Possible partitioning into the aqueous bulk phase and molecular areas were examined by surface activity based mass conservation plots. This shows that the peptide is practically fully accumulated in the interface. Secondary structure and orientation was analyzed by means of polarized infrared reflectivity. Brewster angle microscopy and scanning force microscopy contributed nanostructural images. At low surface pressures the molecules form anti-parallel  $\beta$ -sheets lying flat on the interface. Upon a moderate increase of the lateral pressure a flat  $\beta$ -turn structure appears with inter- and intramolecular H-bonds. We also observed aggregates forming fingerprint-like structures with a diameter of approximately double the hydrophobic length of a  $\beta$ -turn conformation. Beyond approximately  $18 \text{ mN m}^{-1}$  the  $\beta$ -turns straighten up. The lowest measured tilt angle was  $45^\circ$  at  $36 \text{ mN m}^{-1}$ . © 2000 Published by Elsevier Science B.V. All rights reserved.

**Keywords:** HIV-1; Molecular area;  $\beta$ -Turn; Langmuir monolayer; Polarization modulated infrared reflection absorption spectroscopy (PMIRRAS); Brewster angle microscopy (BAM)

\* Corresponding author. Tel.: +41-61-267-2200; fax: +41-61-267-2189.

E-mail address: gerhard.schwarz@unibas.ch (G. Schwarz).

## 1. Introduction

Biomembrane active peptides tend to form a monomolecular film at an air–water interface because of their inherent amphiphilic nature. This can be experimentally studied by means of the conventional Langmuir trough technique [1]. In order to analyze the measured surface activity data quantitatively in terms of the peptide's interfacial area requirement and energetics, the degree of a possible partitioning into the aqueous subphase must be known. However, in cases of a high surface affinity only very small amounts of surfactant (in the nanomolar range) are desorbed in the bulk volume, which are hardly measurable by means of standard analytical methods. Under equilibrium conditions the problem can nevertheless be solved by a novel approach that extrapolates a pertinent set of surface pressure–area data. The procedure is based on thermodynamic principles and has been experimentally tested [2–4].

In such a way, structural information about the interfacial peptide film may be derived from the apparent molecular area, as it depends on the applied lateral pressure. However, this relies mainly on geometric argumentation. Significant complementary information regarding conformation and backbone orientation may be obtained by taking advantage of infrared spectroscopy (for reviews see [5,6]). In the present study we have employed polarization modulated infrared reflection absorption spectroscopy (PMIRRAS) [7–10]. It can be directly applied to a peptide monolayer at an air–water interface under a given surface pressure. Knowing the actual surface concentration of the peptide, the spectroscopic signals may be evaluated towards secondary structure details and tilt angles.

A membrane active agent of most general interest is the so-called fusion peptide, gp41-FP, of HIV-1, i.e. the N-terminal 23-amino acid sequence of the protein subunit gp41 in the viral integral envelope [11]. It is believed to mediate the fusion of the virus with its target cell, a central step in the infection pathway [12]. The structural and thermodynamic properties of the peptide at a border plane between hydrophobic

and hydrophilic moieties like air–water may shed some light on its function in the fusion mechanism.

Previous work [2] has provided some evidence that the peptide at such an interface possibly assumes an  $\alpha$ -helical conformation and changes its orientation from parallel to a more oblique one, an effect that is influenced by the pH of the aqueous surroundings [3]. We have now improved the structural analysis with a slightly modified fusion peptide where *his* takes the place of *met* at position 19. This point mutation would slightly enhance the hydrophilicity of this peptide and is most likely located in the aqueous subphase. Since there are only few amino acid residues reaching into the aqueous subphase, the monolayer properties are still largely dominated by the hydrophobic moiety and the interfacial structure will hardly be affected. The introduction of a histidine allows chemical reactions with that part of the molecule which is located in the aqueous bulk phase. Thus this mutant of gp41-FP will be a valuable tool for further investigations concerning for example its behavior in a lipidic matrix.

Our experimental approach employs a combined thermodynamic/spectroscopic method that is complemented by the use of interfacial microscopy techniques. Brewster angle microscopy (BAM) [13,14] reveals changes in the monomolecular film at a lateral resolution of approximately 10  $\mu\text{m}$  and scanning force microscopy (SFM) can resolve lateral structures in the nanometre range.

## 2. Materials and methods

### 2.1. Substances

The peptide, with the amino acid sequence AVGIGALFLGFLGAAGSTHGARS, was obtained from Genosys Biotechnologies Ltd. (Cambridge, UK). Mass spectroscopy, HPLC analysis and sequence analysis of the peptide, as performed by Genosys, revealed a purity of 98%. Our stock solutions in dimethylsulfoxide (DMSO) (at approx. 1  $\text{mg ml}^{-1}$ ) were stored at  $-18^\circ\text{C}$  in a glass vial with a Teflon septum and argon atmosphere. Concentrations were determined and

checked from time to time by amino acid analysis. Ingredients for the McIlvaine buffer (pH 7.3 and 60 mM ionic strength in the subphase) as well as the DMSO were purchased from Fluka (Buchs, CH). The ultra pure water was prepared with a Millipore apparatus.

## 2.2. Surface activity

Since the peptide is very poorly soluble in water, no useful bulk concentrations can be prepared. Only spreading directly onto the surface leads to equilibrium within a reasonable time. The pressure outside the barriers naturally remains zero during the course of an experiment (as we have verified by measurements). With various given amounts of peptide being spread on the surface of an aqueous bulk volume,  $V$ , the interfacial area,  $A$ , was determined for the same lateral pressure,  $\pi$ , under equilibrium conditions. This implies that the surface concentration,  $\Gamma$ , as well as the concentration in the subphase,  $c_s$ , are invariant. According to mass conservation the total amount per volume becomes

$$c_0 = \Gamma \cdot (A/V) + c_s \quad (1)$$

so that a plot of  $c_0$  vs.  $A/V$  must be linear. Its slope would be equal to the actual surface concentration, whereas the intercept on the  $c_0$ -axis reflects the subphase concentration. The underlying theoretical basis and an appropriate experimental procedure involving conventional pressure–area isotherms have been described previously in great detail [2]. The active trough area was not corrected for the Wilhelmy plate effect [15] since the dimensions of the Wilhelmy platelet relative to the trough area made it negligible.

In the present study three computer-interfaced rectangular Teflon film balances (from Nima, Coventry, UK) were used: (i) a Nima 610 with one moving barrier (dimensions:  $30 \times 10$  cm,  $V = 176$  cm<sup>3</sup>); (ii) a microtrough system, Nima 301M ( $7 \times 14$  cm,  $V = 61$  cm<sup>3</sup>) having two moving barriers; and (iii) a Nima 6100 ( $30 \times 10$  cm,  $V = 280$  cm<sup>3</sup>) equipped with dipping facilities. In addition a set of constant area troughs, manufactured in the Biocenter workshop, was used for measurements

at constant area (isochoric mode). Trough preparation and handling, the checking of equilibrium conditions and performing of measurements are comprehensively described in previous publications [2–4]. Prior to any measurement series the trough area and the film balance were calibrated. Isotherms were recorded with a barrier speed of  $5\text{--}8$  cm<sup>2</sup> min<sup>−1</sup>. All troughs had been enclosed by a box to avoid contamination. In addition the box covering the Nima 301M was saturated with humid air to minimize evaporation, and the constant area troughs and the Nima 6100 were equipped with a Level-O-matic (NFT, Göttingen, Germany) which adjusts the water level in the trough. The subphase of all troughs was stirred with tiny magnetic stirrers. Small volumes of peptide stock solution were carefully deposited onto the surface by a microsyringe (Hamilton, Bonaduz, CH).

## 2.3. PMIRRAS measurements

It has recently been shown that a differential mode of infrared reflectivity measurements by polarization modulation of the incident light (PMIRRAS) can quite effectively yield a profitable vibrational spectrum of a surfactant monolayer at the air–water interface [7–10]. In the case of peptide films, the observed intensities of especially the amide I and amide II bands may be analyzed with regard to the existing secondary structure and backbone orientation [16,17]. In particular, the characteristic frequency of the amide I mode is situated in the range  $1650\text{--}1660$  cm<sup>−1</sup> for an  $\alpha$ -helix, near  $1630$  cm<sup>−1</sup> for a parallel  $\beta$ -sheet and in the range  $1670\text{--}1680$  cm<sup>−1</sup> for a  $\beta$ -turn. For an antiparallel  $\beta$ -sheet the amide I mode is split into a strong band in the range  $1620\text{--}1630$  cm<sup>−1</sup> and a weaker one near  $1690$  cm<sup>−1</sup>.

For our PMIRRAS measurements only the Nima 301M trough was used. Stirring and barrier movements were stopped during the measurement of the spectra. These were recorded by a Nicolet 740 interferometer with a spectral resolution of  $4$  cm<sup>−1</sup> taking 300 or 200 scans per spectrum. At a higher level of compression the film pressure tended to decrease to some extent when the barriers were stopped for the recording

of the IR spectra, these were assigned to an appropriate average film pressure,  $\langle \pi \rangle$ . The lateral pressure decreased, for example from 10.2 to 9.3 mN m<sup>-1</sup> in 15 min, corresponding to  $\langle \pi \rangle = 9.7$  mN m<sup>-1</sup>.

#### 2.4. BAM measurements

Morphological images of the monolayers were taken by means of a home-designed Brewster angle microscope (a gift from Hoechst AG, Germany) which was positioned over the Nima 6100 trough. The light source of the BAM was a He–Ne laser. After striking the buffer surface at the Brewster angle (minimal intensity) the laser beam was reflected at a mirror and recorded by a CCD camera [18]. A video system was used for data storage.

#### 2.5. SFM measurements

From the Nima 6100 trough the films were transferred by means of the Langmuir–Blodgett technique to freshly cleaved mica at a speed of 2 mm min<sup>-1</sup>. Images were taken at three sufficiently different spots of each film. In all cases the images obtained at one fixed surface pressure gave practically the same results. The films were inspected with a commercial SFM instrument (NanoScope III, Multimode™, Digital Instrument, Santa Barbara, CA) equipped with Si cantilevers of 127  $\mu$ m length with a resonance frequency of 250–350 kHz purchased from Nanosensors (Wetzlar-Blankenfeld, Germany). The topographical data were taken in the ‘tapping mode™, (intermittent contact) [19]. All the experiments were performed at room temperature and atmospheric pressure.

### 3. Results

#### 3.1. Surface activity

Pressure–area isotherm measurements were carried out with a large series of spread peptide

amounts (in the nanomole range). The rate of area compression (set by the barrier speed) was sufficiently low to assure equilibrium between the monolayer and subphase domains being confirmed by isochoric tests [2]. Mass conservation plots according to Eq. (1) for given surface pressures were performed up to 36 mN m<sup>-1</sup>. Two examples are displayed in Fig. 1. In any case straight lines are obtained that can be extrapolated through the origin within the margin of experimental uncertainty. Thus a desorption of peptide into the bulk volume can be practically neglected. The partial molecular areas,  $a_p$ , shown in Fig. 2, have therefore been calculated with the total amount of spread peptide. With increasing lateral pressure the area requirement of the peptide decreases. Taking into account the pH dependence of the wild type (wt) peptide [3], the mutant and wt peptides do exhibit practically the same degree of surface activity. Assuming an approximately cylindrical shape of the peptide molecule, the decrease of molecular area by a factor of 0.7 upon the transition is used for a geometrically based estimation of the tilt angle resulting in 45°, which is in line with the infrared data (see below).

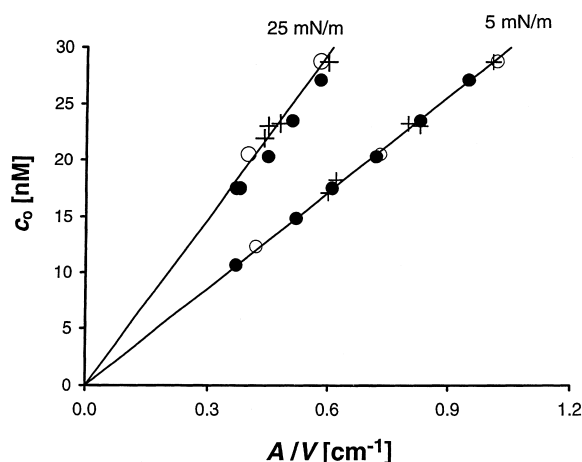


Fig. 1. Mass conservation plots. Total concentration is plotted vs. film area per subphase volume for 5 and 25 mN m<sup>-1</sup>. Different symbols indicate data from different measurement series

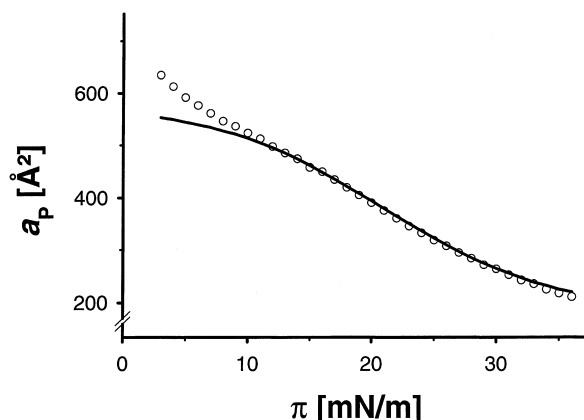


Fig. 2. Change of the interfacial molecular area requirement of the present mutant of gp41-FP with film pressure ( $\circ$ ). The results obtained by the wt (solid curve) are fitted with the following parameters:  $a_0 = 580 \text{ Å}^2$ ,  $a_\infty = 180 \text{ Å}^2$ ,  $\pi_0 = 6.8 \text{ mN m}^{-1}$ ,  $\pi^* = 21 \text{ mN m}^{-1}$  (see [2])

### 3.2. Infrared spectroscopy

PMIRRAS spectra of the peptide monolayer at the water surface were recorded with increasing surface pressures from 1.6–36  $\text{mN m}^{-1}$  (Fig. 3). The spectra have been corrected for the baseline and the peptide concentration at the air–water

interface,  $\Gamma$ , which can be derived from  $a_p$  according to

$$\Gamma = (a_p \cdot N_A)^{-1} \quad (2)$$

These spectra have been decomposed into their components in order to follow the intensity variation with the surface pressure. From Fig. 3, some spectral modifications can be clearly derived: (i) there is a shift of the amide I maximum from  $1620.3 \text{ cm}^{-1}$  towards  $1628.2 \text{ cm}^{-1}$  with increasing  $\pi$ . Details are presented in Fig. 4 where the maximum of the amide I band increases until  $\pi$  reaches approximately  $18 \text{ mN m}^{-1}$  and then remains almost constant. The amide I band is representative for  $\beta$ -strand structures of the peptide backbone. (ii) The shape of the amide I spectral region drastically changes with  $\pi$ . At low surface pressures bands characteristic of anti-parallel  $\beta$ -sheets (at  $1620$  and  $1698 \text{ cm}^{-1}$ ) are almost exclusively observed. Then beyond  $6 \text{ mN/m}$  a new component appears in the  $1640$ – $1670 \text{ cm}^{-1}$  range. (iii) The spectra also exhibit some intensity variation for both the amide I and amide II bands. The magnitudes of these variations are shown in Fig.

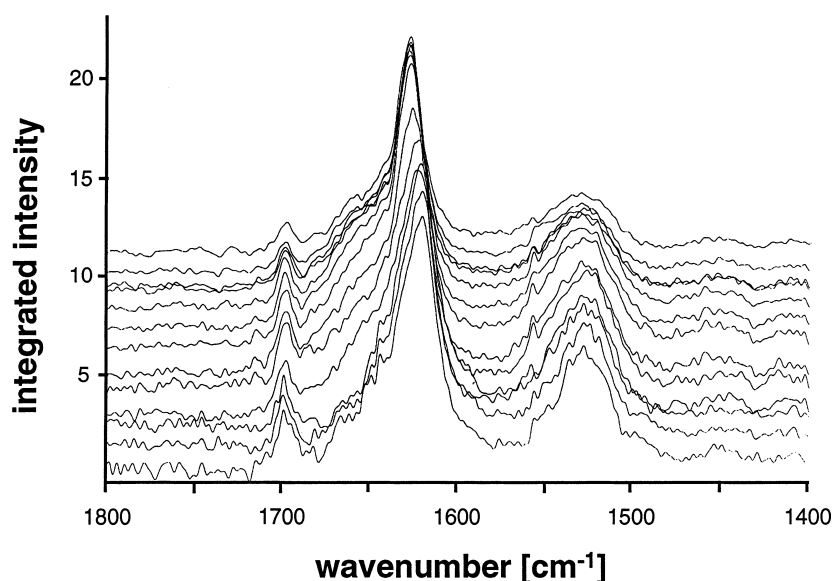


Fig. 3. PMIRRAS spectra of the mutant of gp41-FP (13 out of 19 are shown). The lateral pressures from bottom to top are:  $\pi/(\text{mN m}^{-1}) = 1.6; 4.1; 6.1; 6.5; 9; 14.5; 17; 19; 21; 25; 28; 33; \text{ and } 36$

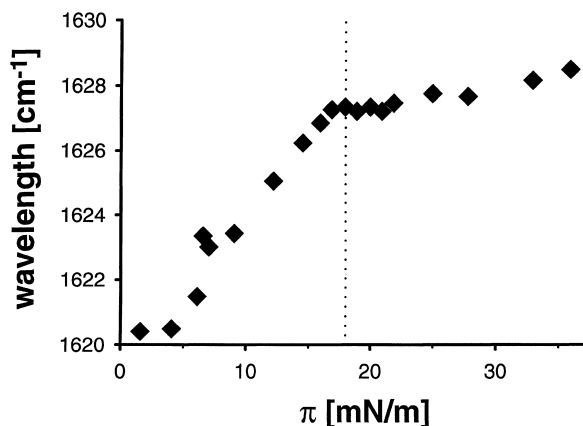


Fig. 4. Shift of the peak maximum of the amide I band with increasing lateral pressure as derived from Fig. 3. The dotted line indicates  $18 \text{ mN m}^{-1}$ .

5. Different features in regions at low and high lateral pressures can also be clearly distinguished here. The apparent sharp bend of the integrated intensity of the  $1698$  and  $1625 \text{ cm}^{-1}$  bands (Fig. 5a) as well as the total amide I band, i.e. the sum of all the secondary structure components (Fig. 5b), again occurs at about  $18 \text{ mN m}^{-1}$ . For the amide II band (Fig. 5c) there is no splitting in the low pressure or the high pressure range. Conformational analysis of the amide I and amide II bands suggests a  $\beta$ -turn structure in both ranges. However, under low pressure the peptide is oriented mainly parallel to the interface, while upon application of higher pressure its orientation becomes more and more oblique. From our estimation, the angles between the axes parallel and perpendicular to the chain direction and the plane of the surface are approximately  $30^\circ$  and  $35^\circ$ , respectively. This leads to a dihedral angle between the surface plane and the sheet plane of  $45^\circ$ .

### 3.3. Brewster angle microscopy

At non-measurable low surface pressures below  $0.1 \text{ mN m}^{-1}$  the peptide already forms pronounced aggregates at the interface. These aggregates accumulate and form a smooth continuous non-structured film. The texture of this film re-

mains unaltered up to approximately  $18 \text{ mN m}^{-1}$ . Then parts of the film suddenly display a rougher appearance. BAM images (Fig. 6) taken at  $10$  and  $25 \text{ mN m}^{-1}$  exemplify these two textures. The left image resembles the low-pressure region with its

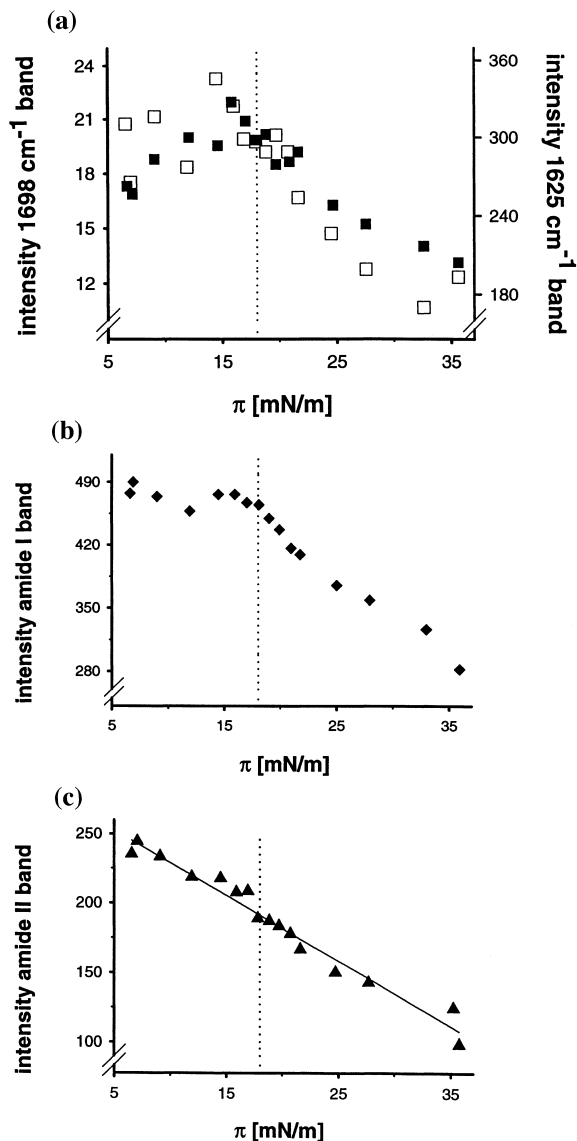


Fig. 5. Variation of the integrated intensities with surface pressure: (a) the band at  $1698 \text{ cm}^{-1}$  ( $\square$ ) and the  $1625 \text{ cm}^{-1}$  band ( $\blacksquare$ ); (b) the whole amide I band; (c) the amide II band. The dotted lines indicate  $18 \text{ mN m}^{-1}$ . For the amide II band no pronounced alteration at  $18 \text{ mN m}^{-1}$  can be observed.

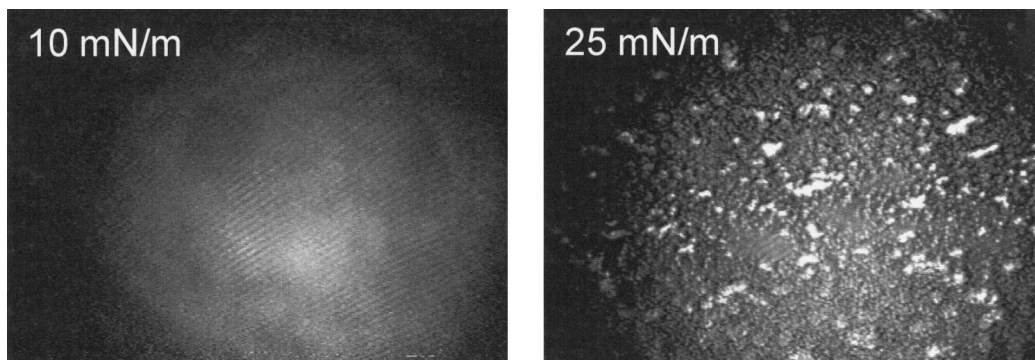


Fig. 6. BAM pictures of the present mutant of gp41-FP at the air–water interface taken at 10 and 25  $\text{mN m}^{-1}$ . The sections have the dimensions of 1  $\text{mm}^2$ , thus the pictures are a little bit distorted. Left part: ‘smooth texture’; right part: ‘landscape texture’

smooth appearance, the right one shows an area with the rougher ‘landscape texture’ occurring beyond approximately 18  $\text{mN m}^{-1}$ . The areas with the ‘landscape texture’ increase with increasing lateral pressure.

#### 3.4. Scanning force microscopy

SFM images of the low pressure region at 10  $\text{mN m}^{-1}$  and of the high pressure region at 25  $\text{mN m}^{-1}$  have been recorded. Both show the

peptide arranged in fingerprint-like structures. The stripes can reach lengths of over 500 nm. Fig. 7 displays SFM images at 10 and 25  $\text{mN m}^{-1}$ . At 10  $\text{mN m}^{-1}$  the width of the stripes is in the range 5–7 nm and the distance between the stripes is approximately 10 nm. At 25  $\text{mN m}^{-1}$  the stripes have a broader width of 4–8 nm and the distance between two stripes has become approximately 7–8 nm. With the wt peptide we have also tried to transfer a film onto other substrates, especially  $\text{SiO}_2$  [Taylor et al., unpublished results]. In that

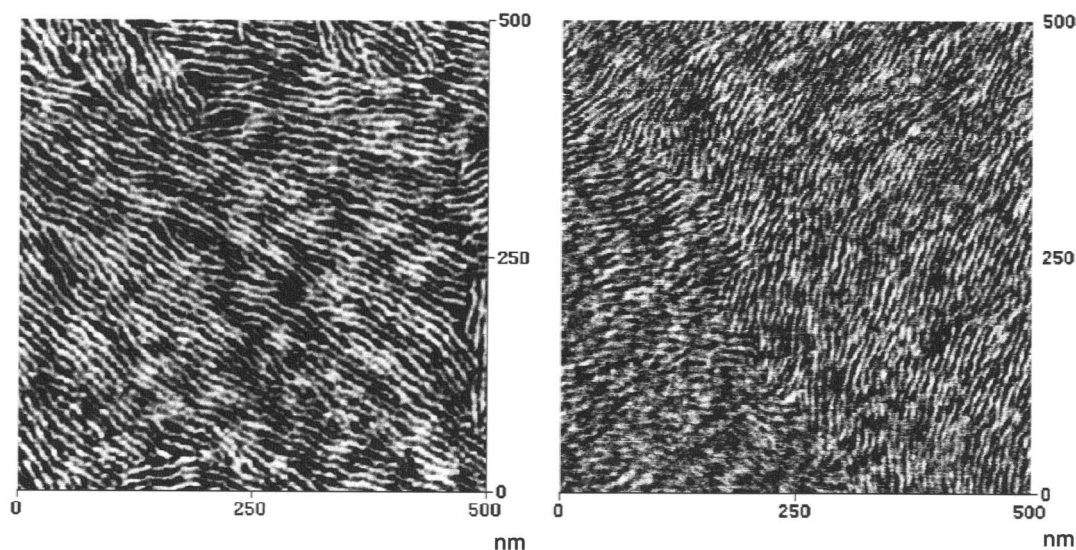


Fig. 7. SFM phase pictures of the mutant of gp41-FP (transferred on mica) taken at 10  $\text{mN m}^{-1}$  (left side) and 25  $\text{mN m}^{-1}$  (right side).

case similar structures were observed as for those on mica, although the image was not as good (due to the roughness of  $\text{SiO}_2$ ). Accordingly, we think that the structure is substrate-independent.

#### 4. Discussion

We have investigated the structural behavior of a mutant of the fusion peptide of HIV-1 at the air–water interface. In the wt amino acid sequence a methionine at position 19 was replaced by a histidine. The surface activity of this mutant is very similar to that of the wt peptide. The  $\pi$  vs.  $A$ -isotherms of both show an inflection in their course, which occurs at approximately the same lateral pressure if the pH dependence of the wt peptide is taken into account.

On the basis of computer modeling it was previously proposed that at low pressure the wt peptide assumes the structure of an  $\alpha$ -helix being oriented parallel to the interface [2]. However, a  $\beta$ -turn motif lying flat onto the surface would require the same cross-sectional area of approximately  $600 \text{ \AA}^2$ . Therefore the pressure–area experiments cannot distinguish between these two structures. The same holds true for the mutant, since the replacement of *met* with *his* does not alter the respective cross sectional areas as calculated by molecular modeling of ideal structures. The reduced area requirements in the high pressure region for the mutant can be explained by a straightening up of the low pressure structure to an oblique orientation relative to the surface normal, as also observed for the wt [2], for melittin [4,20] or gramicidin [21]. The results derived from the surface activity confirm our presumption that the point mutation *met*  $\rightarrow$  *his* does not significantly affect the interfacial properties.

Whether the mutant of gp41-FP at the air–water interface adopts an  $\alpha$ -helical or a  $\beta$ -turn structure can be decided by PMIRRAS spectroscopy. The data obtained with this technique revealed almost exclusively anti-parallel  $\beta$ -sheets without any detectable absorption coming from other secondary structures at low surface pressures ( $\pi < 6 \text{ mN m}^{-1}$ ). This implies that they are

intermolecular sheets. Moreover, the intensity ratio (approx. 12) between the  $1620$  and  $1698 \text{ cm}^{-1}$  bands indicates that these sheets lie flat on the surface. Thus an  $\alpha$ -helical structure, which would give an absorption band located near  $1650 \text{ cm}^{-1}$ , can be ruled out.

For moderate pressures of  $6$ – $18 \text{ mN m}^{-1}$  the position of the amide I maximum shifts from  $1620.3$  to  $1627.5 \text{ cm}^{-1}$  (see Fig. 4) indicating a modification of the nature of the  $\beta$ -sheets. Moreover, the intensities of the two components at  $1698$  and  $1620$ – $1625 \text{ cm}^{-1}$  remain practically constant in this pressure range (see Fig. 5a). In addition, the appearance of a shoulder in the  $1640$ – $1670 \text{ cm}^{-1}$  range was noted, which can be assigned to  $\beta$ -turns. This suggests the formation of inter- and intramolecular H-bonds between the  $\beta$ -strands. This model explains both the frequency shift and the intensity behavior.

Beyond the moderate pressure range a change is observed in the appearance of the curves presented in Fig. 5a,b. The apparent intensity variations can be directly connected to a change in the orientation of the  $\beta$ -sheets with respect to the surface. According to the PMIRRAS selection rule, the intensity decrease of the  $1620$ – $1625$  and the  $1698 \text{ cm}^{-1}$  bands indicates a rotation of the  $\beta$ -sheets plane around the axes parallel and perpendicular to the chain direction, respectively.

The lowest tilt angle of the peptide molecules relative to the surface normal as estimated from the PMIRRAS experiments was approximately  $45^\circ$ , which is in good agreement with the calculations based on the surface activity measurements.

The images obtained by Brewster angle microscopy also support a change in the film topography beyond  $18 \text{ mN m}^{-1}$ . At that surface pressure small domains with a landscape-like texture can be observed, which become enlarged with increasing  $\pi$ . The brightness of this texture compared to the ‘smooth texture’ of the low-pressure range may indicate that the film in those domains has a greater thickness, which is consistent with a decrease in the tilt angle as found in the PMIRRAS experiments. However BAM experiments alone cannot prove this since the change in the texture could also be explained by a change in the azimuth of the peptide backbone.



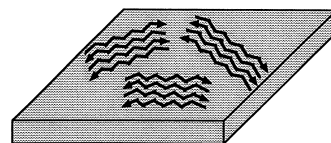
On first glance the SFM images of the low pressure region and the high pressure region look similar. Both resemble long parallel oriented stripes. Stripe-like structures have also been observed in other Langmuir–Blodgett films, e.g. some dihydroxy-alkane carbonic acid esters [22]. A closer look at the images obtained for the present mutant of gp41-FP reveals that the stripes are more closely packed at  $25 \text{ mN m}^{-1}$  compared to  $10 \text{ mN m}^{-1}$ . This is mainly an effect of the stripe distance, which increases by 2–3 nm. It is reasonable to assume that the space between the stripes is occupied by the hydrophilic parts of the peptide, which are charged at the pH we used. Thus coulomb repulsion is likely to play a major role in the characteristics of the space between the stripes and can only partly be overcome by lateral compression. The increase in the range of the stripe width by approximately 2 nm even though the peptides are tilted when  $\pi$  increases beyond  $18 \text{ mN m}^{-1}$  is most likely an effect of the cantilever tip.

Based mainly on our data and interpretations derived from the PMIRRAS and surface activity measurements (which are quite compatible with BAM and SFM) the model schematically proposed in Fig. 8 would explain the present results: At very low pressures ( $< 6 \text{ mN m}^{-1}$ ) the peptide adopts the structure of antiparallel  $\beta$ -sheets lying flat in the interface. Between 6 and  $18 \text{ mN m}^{-1}$  the intermolecular hydrogen bonds are broken and intramolecular hydrogen bonds are formed. This rearrangement is accompanied by the formation of  $\beta$ -turns. At pressures above  $18 \text{ mN m}^{-1}$  the  $\beta$ -turn structures then straighten up.

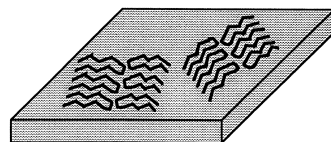
## 5. Conclusions

A point mutation *met*  $\rightarrow$  *his* in the wt fusion peptide of HIV-1 does not substantially change the interfacial surface activity of the peptide. Upon molecular compression the structure of the peptide undergoes apparent transitions along the following lines:

$\pi < 6 \text{ mN/m}$



$6 < \pi < 18 \text{ mN/m}$



$\pi > 18 \text{ mN/m}$

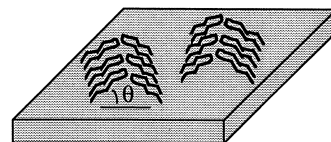


Fig. 8. Sketches of the different interfacial structures apparently adopted by the peptide during compression. The angle  $\theta$  indicates that the peptide's backbone reaches out of the plane of the surface.

- Below  $6 \text{ mN m}^{-1}$  the peptide mainly forms intermolecular anti-parallel  $\beta$ -sheets with their backbones lying flat in the interface (see sketch 1 in Fig. 8).
- For  $6$ – $18 \text{ mN m}^{-1}$ , corresponding to the phase transition on the isotherm, the peptides fold into clips leading to both inter- and intramolecular anti-parallel  $\beta$ -sheets (see sketch 2 in Fig. 8). During this transition the plane of the sheets does not change its orientation relative to the interface.
- Beyond  $18 \text{ mN m}^{-1}$  the structure remains unaltered, but there is a continuous change of orientation of the  $\beta$ -sheets plane as the surface pressure increases. At the highest pressure ( $36 \text{ mN m}^{-1}$ ), the tilt angle of this plane with respect to the surface normal is approximately  $45^\circ$  (see sketch 3 in Fig. 8).

Possible parallel  $\beta$ -sheets during and after the phase transition can definitely be neglected compared with the anti-parallel species.

## Acknowledgements

This research has been supported by the Swiss National Science Foundation grant No. 31-42045.94 (to G. Schwarz), the German Research Foundation (to H. Fuchs) and a Lise–Meitner Stipendium (to L.F. Chi).

## References

- [1] H. Kuhn, D. Möbius, Monolayer assemblies, in: B.W. Rossiter, R.C. Baetzold (Eds.), *Investigations of Surfaces and Interfaces-Part B*, Physical Methods of Chemistry, IXB, 2nd edition, J Wiley and Sons, New York, 1993, pp. 375–542.
- [2] G. Schwarz, S.E. Taylor, Thermodynamic analysis of the surface activity exhibited by a largely hydrophobic peptide, *Langmuir* 11 (1995) 4341–4346.
- [3] S.E. Taylor, G. Schwarz, The molecular area characteristics of HIV-1 gp41 fusion peptide at the air–water interface. Effect of pH, *Biochim. Biophys. Acta* 1362 (1997) 257–264.
- [4] G. Wackerbauer, I. Weis, G. Schwarz, Preferential partitioning of melittin into the air–water interface. Structural and thermodynamic implications, *Biophys. J.* 71 (1996) 1422.
- [5] L.K. Tamm, S.A. Tatulian, Infrared spectroscopy of proteins and peptides in lipid bilayers, *Quart. Rev. Biophys.* 30 (1997) 365–429.
- [6] E. Goormaghtigh, V. Raussens, J.-M. Ruyschaert, Attenuated total reflection spectroscopy of proteins and lipids in biological membranes, *Biochim. Biophys. Acta* 1422 (1999) 105–185.
- [7] D. Blaudez, T. Buffeteau, J.C. Cornut, B. Debat, N. Escafre, M. Pézolet, J.M. Turllet, Polarization-modulated FT-IR spectroscopy of a spread monolayer at the air–water interface, *Appl. Spectrosc.* 47 (1993) 869–874.
- [8] D. Blaudez, T. Buffeteau, J.C. Cornut, B. Debat, N. Escafre, M. Pézolet, J.M. Turllet, Polarization modulation FT-IR spectroscopy at the air–water interface, *Thin Solid Films* 242 (1994) 146–150.
- [9] I. Cornut, B. Desbat, J.M. Turllet, J. Dufourcq, In situ study by polarization modulated FTIR spectroscopy of the structure and orientation of lipids and amphipatic peptides at the air–water interface, *Biophys. J.* 70 (1996) 305–312.
- [10] D. Blaudez, J.M. Turllet, J. Dufourcq, D. Bard, T. Buffeteau, B. Desbat, Investigations at the air–water interface using polarization modulation infrared spectroscopy, *J. Chem. Soc. Faraday Trans.* 92 (1996) 525–530.
- [11] W.R. Gallaher, Detection of a fusion peptide sequence in the transmembrane protein of human immunodeficiency virus, *Cell* 50 (1987) 327–328.
- [12] H. Schaal, M. Klein, P. Gehrmann, O. Adams, A. Scheid, Requirement of N-terminal amino acid residues of gp41 for human immunodeficiency virus type 1-mediated cell fusion, *J. Virol.* 69 (1995) 3308–3314.
- [13] S. Hénon, J. Meunier, Microscope at the Brewster angle: direct observation of the first-order phase transition in monolayers, *Rev. Sci. Instrum.* 62 (1991) 936–939.
- [14] D. Hönig, D. Möbius, Direct visualization of monolayers at the air–water interface by Brewster angle microscopy, *J. Phys. Chem.* 95 (1991) 4590–4592.
- [15] P.B. Welzel, I. Weis, G. Schwarz, Sources of error in Langmuir trough experiments. Wilhelmy plate effects and surface curvature, *Colloids Surf. A: Physicochem. Eng. Aspects* 144 (1998) 229–234.
- [16] T. Miyazawa, Infrared spectra and helical conformations, in: G.D. Fasman (Ed.), *Poly- $\alpha$ -Amino Acids*, Marcel Dekker, New York, 1967, pp. 69–103 (chapter 2).
- [17] E. Goormaghtigh, V. Cabiaux, J.M. Ruyschaert, Physical methods in the study of biomembranes, in: H.J. Hilderson, G.B. Ralston (Eds.), *Subcellular Biochemistry*, 23, Plenum Press, 1994, pp. 342–357 (chapter 8).
- [18] S. Jacobi, L.F. Chi, M. Plate, M. Overs, H.-J. Schäfer, H. Fuchs, Monolayer studies of methyl vic-dihydroxyoctadecanoates, *Thin Solid Films* 327–329 (1998) 180–184.
- [19] Q. Zhong, D. Innis, K. Kjoller, V.B. Elings, Fractured polymer–silica fiber surface studied by tapping mode atomic force microscopy, *Surf. Sci.* 290 (1993) 688–692.
- [20] K.S. Birdi, V.S. Gevod, O.S. Ksenzhek, E. Stenby, K.L. Rasmussen, Equation of state for monomolecular films of melittin at air–water interface, *Colloid Polym. Sci.* 261 (1983) 767–775.
- [21] A. Dhathathreyan, U. Baumann, A. Müller, D. Möbius, Characterization of complex gramicidin monolayers by light reflection and Fourier transform infrared spectroscopy, *Biochim. Biophys. Acta* 944 (1988) 265–272.
- [22] L.F. Chi, S. Jacobi, B. Anczykowski, M. Overs, H.-J. Schäfer, H. Fuchs, Supramolecular periodic structures in monolayers, *Adv. Mater.* 12 (2000) 25–30.